

A Mass Spectrometric Determination of the Conformation of Dimeric Apolipoprotein A-I in Discoidal High Density Lipoproteins[†]

R. A. Gangani D. Silva,[‡] George M. Hilliard,[§] Ling Li,^{||,⊥} Jere P. Segrest,^{||,⊥,#} and W. Sean Davidson^{*·‡}

Department of Pathology and Laboratory Medicine, The University of Cincinnati, Cincinnati, Ohio 45237, Department of Molecular Sciences and Center of Excellence in Genomics and Bioinformatics, University of Tennessee Health Science Center, Memphis, Tennessee 38163, and Department of Medicine, Atherosclerosis Research Unit, and Department of Biochemistry and Molecular Genetics, UAB Medical Center, Birmingham, Alabama 35294

Received March 4, 2005; Revised Manuscript Received April 26, 2005

ABSTRACT: Discoidal forms of high density lipoproteins (HDL) are critical intermediates between lipid-poor apolipoprotein A-I (apo A-I), the major protein constituent of HDL, and the mature spherical forms that comprise the bulk of circulating particles. Thus, many studies have focused on understanding apoA-I structure in discs reconstituted *in vitro*. Recent theoretical and experimental work supports a “belt” model for apoA-I in which repeating amphipathic helical domains run parallel to the plane of the lipid disc. However, disc-associated apoA-I can adopt several tertiary arrangements that are consistent with a belt orientation. To distinguish among these, we cross-linked near-neighbor Lys groups in homogeneous 96 Å discs containing exactly two molecules of apoA-I. After delipidation and tryptic digestion, mass spectrometry was used to identify 9 intermolecular and 11 intramolecular cross-links. The cross-linking pattern strongly suggests a “double-belt” molecular arrangement for apoA-I in which two apoA-I molecules wrap around the lipid bilayer disc forming two stacked rings in an antiparallel orientation with helix 5 of each apoA-I in juxtaposition (LL5/5 orientation). The data also suggests the presence of an additional double-belt orientation with a shifted helical registry (LL5/2 orientation). Furthermore, a 78 Å particle with two molecules of apoA-I fit a similar double-belt motif with evidence for conformational changes in the N-terminus and the region near helix 5. A comparison of this work to a previous study is suggestive that a third molecule of apoA-I can form a hairpin in larger particles containing three molecules of apoA-I.

It is well accepted that increased plasma high density lipoprotein (HDL)¹ levels reduce the risk of atherosclerosis, a leading cause of coronary artery disease (CAD) (1). Although it has many antiatherogenic functions, the proposed ability to transport excess cellular cholesterol from the periphery to the liver is the best recognized HDL function (2, 3). Apolipoprotein A-I (apoA-I) is the major HDL protein

constituent and a critical mediator of this reverse cholesterol transport (RCT) process (4). ApoA-I may adjust its conformation in different HDL subclasses to optimize interaction with plasma and membrane proteins at appropriate steps in the pathway. Therefore, knowledge of the tertiary relationships of apoA-I molecules with respect to each other in HDL is required to fully understand HDL function.

Although of low abundance in plasma, discoidal HDL particles represent critical intermediates between lipid-poor apoA-I and mature spherical HDL that comprise the bulk of circulating particles. The structure of apoA-I-containing discs has been hotly debated for three decades, but it is fair to say that most recent studies support a “belt” orientation originally proposed by Segrest (5, 6). The basic criterion of the model holds that the main lipid binding structures of apoA-I, 10 repeating amphipathic α -helical domains, surround a unilamellar phospholipid bilayer such that the helices are oriented parallel to the plane of the disc and perpendicular to the lipid acyl chains (reviewed in ref 7). The belt model is supported by a crystal structure of a deletion mutant of apoA-I ($\Delta 1-43$ apoA-I) that adopted a distorted ring shape, although in the absence of lipids (8). More direct support for a belt orientation was obtained by polarized internal reflection infrared spectroscopy (9) and fluorescence quenching experiments (10, 11).

[†] This work was supported by Grants HL67093 and HL62542 (W.S.D.) from the NIH and a postdoctoral fellowship from the Ohio Valley Affiliate of the American Heart Association (R.A.G.D.S.).

* To whom correspondence should be addressed. Mailing address: Department of Pathology and Laboratory Medicine, University of Cincinnati, 2120 Galbraith Rd., Cincinnati, OH 45237-0507. Tel: (513) 558-3707. Fax: (513) 558-1312. E-mail: Sean.Davidson@UC.edu.

[‡] The University of Cincinnati.

[§] University of Tennessee Health Science Center.

^{||} Department of Medicine, UAB Medical Center.

[⊥] Atherosclerosis Research Unit, UAB Medical Center.

[#] Department of Biochemistry and Molecular Genetics, UAB Medical Center.

¹ Abbreviations: apoA-I, apolipoprotein A-I; BS³, (bis)sulfosuccinimidyl suberate; DSP, dithiobis (succinimidylpropionate); CAD, coronary artery disease; FPLC, fast performance liquid chromatography; HDL, high density lipoprotein; HPLC, high performance liquid chromatography; MS, mass spectrometry; MWCO, molecular weight cutoff; TIC, total ion chromatogram; PBS, phosphate buffered saline; POPC, 1-palmitoyl-2-oleoyl-*sn*-glycero-3-phosphatidylcholine; RCT, reverse cholesterol transport; RP-HPLC, reversed-phase HPLC; SDS-PAGE, sodium dodecyl sulfate-polyacrylamide gradient gel electrophoresis.

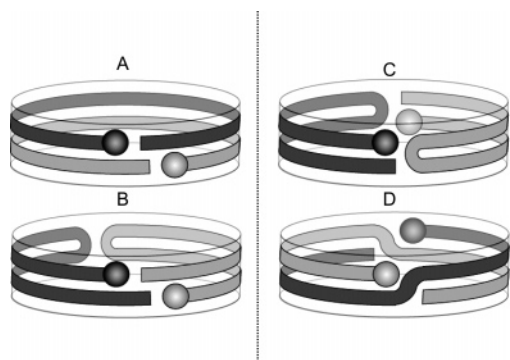


FIGURE 1: Belt models proposed for apoA-I on the edge of discoidal HDL particles that contain two molecules of apoA-I. Two protein molecules in each model are shown as belts of two shades of gray. The N-terminal 43 residues, which do not fit the typical amphipathic helical repeat structure apoA-I, are shown as a sphere at the N-terminus of each molecule. Panel A: Segrest's double-belt model (12). Panel B: hairpin model, head-to-head arrangement. Panel C: hairpin model, head-to-tail arrangement. Panel D: Z-belt model (11).

In terms of tertiary structure, the most detailed hypothesis for apoA-I as a belt is the “double-belt” model. It holds that two ring shaped apoA-I molecules are stacked in an antiparallel arrangement (Figure 1A), each occupying a leaflet of the lipid bilayer. In this configuration there are two possible interfaces between the molecules depending on how they are stacked: left to left (LL), and right to right (RR). Computer analysis indicated that an LL interface in which helix 5 (more specifically, glycine 129) of each molecule is directly opposed to helix 5 (glycine 129) of the other produced the highest weighted score of potential salt bridges between the apoA-I molecules (12). This is called the LL5/5 (G129j) registry and, interestingly, is the same orientation found in the crystal structure (8). However, there are other possible belt arrangements including hairpins that can be either head-to-head or head-to-tail (Figure 1B,C) (13). These preserve the same salt bridge interactions as the double belt, although they are intramolecular in the hairpins. A “Z-belt” model was also suggested because of its symmetry (Figure 1D) (10).

To date, no study has unequivocally distinguished between the models depicted in Figure 1. We recently addressed this problem using high resolution mass spectrometry combined with cross-linking chemistry (14). The results strongly supported the existence of the salt bridge interactions proposed for the double-belt model. However, we were unable to distinguish between the double-belt model and the head-to-head hairpin arrangement as cross-links were found that fit both models. In the current study, we hypothesized that a contaminating trimeric form of apoA-I resulting from heterogeneity in our original disc preparations may have created ambiguities in our original study. Using an optimized reconstitution procedure, we eliminated structural heterogeneity in the particles and used a different cross-linking agent to increase the number of linkages capable of distinguishing between the models. We show that the double-belt form predominates in 96 Å diameter particles containing exactly two molecules of apoA-I. A variation of this same model also holds for smaller 78 Å complexes.

EXPERIMENTAL PROCEDURES

ApoA-I Purification and Preparation of rHDL Particles. Human apoA-I isolation and purification from normal human plasma was carried out as reported previously (14, 15). The Bio-bead cholate removal method was used for the preparation of reconstituted HDL (rHDL) discs as reported (10). Phospholipid, 1-palmitoyl-2-oleoyl-*sn*-glycero-3-phosphatidylcholine (POPC, Avanti Polar Lipids, Birmingham, AL), and free unesterified cholesterol (FC, Sigma, St. Louis, MO) were used in the particle reconstitution. A molar ratio of 78:4:1 POPC:FC:apoA-I was used in 96 Å particle construction, and 35:2:1 POPC:FC:apoA-I was used for the 78 Å particle preparations. To remove unreacted apoA-I and lipids, HDL preparations were purified using a tandem gel filtration column system (Superdex 200 and Superose 6, Amersham Biosciences, Piscataway, NJ) equilibrated in phosphate buffered saline (PBS, pH 7.8), controlled by a fast performance liquid chromatography system (Amersham Biosciences). The homogeneity of the particles was confirmed by a native 8–25% polyacrylamide Phast gel (Amersham) just prior to cross-linking.

Cross-Linking and Tryptic Digestion of apoA-I. Freshly prepared bis(sulfosuccinimidyl) suberate (BS³) cross-linker (6.5 mg/mL in PBS, pH 7.8, Pierce, Rockford, IL) was added to homogeneous rHDL (1 mg/mL apoA-I concentration) at a protein to BS³ molar ratio of 1:10. The BS³ solution preparation and addition to the protein solution was done within 1 min to minimize hydrolysis of the cross-linker. Samples were incubated at 4 °C for 24 h. The samples were lipid extracted using standard chloroform/methanol extraction procedures as reported previously (14). The cross-linked protein was solubilized in standard Tris buffer containing 3 M guanidine and separated into monomeric (~28.1 kDa) and dimeric (~56.2 kDa) protein components using the two gel filtration column setup described above, equilibrated in the same buffer. Fractions corresponding to the dimer and the monomer were pooled separately, dialyzed into 5 mM ammonium bicarbonate, and concentrated by ultrafiltration (YM-10, Millipore Corporation, Bradford, MA). The protein samples were digested using 5% w/w sequencing grade trypsin (Promega) to protein for 2 h at 37 °C, lyophilized, and stored at –20 °C until used for mass spectrometry.

Mass Spectrometry and Data Analysis. Peptide mass detection was carried out on a Sciex QSTAR DE spectrometer (equipped with an electrospray ionizer and a quadrupole time-of-flight dual analyzer) connected to a capillary HPLC (Agilent 1100) capable of doing on-line peptide separations. Liquid chromatography (LC) mass spectrometry (MS) experimental conditions including LC peptide elution and peptide mass detection techniques used in the current experiment were similar to those of the previous study (14). In brief, individual mass spectra corresponding to the each peak in the total ion chromatogram (TIC, the detector response for the masses reaching the detector as a function of time) were generated, and monoisotopic masses were calculated averaging different charge states corresponding to the same mass. The resulting list of tryptic peptides was analyzed by GPMW (ChemSW, Inc.) to assign sequence identity of individual peptides with or without a modification by a cross-linker. The putative amino acid sequence identities of the intra/intermolecularly cross-linked peptide masses were

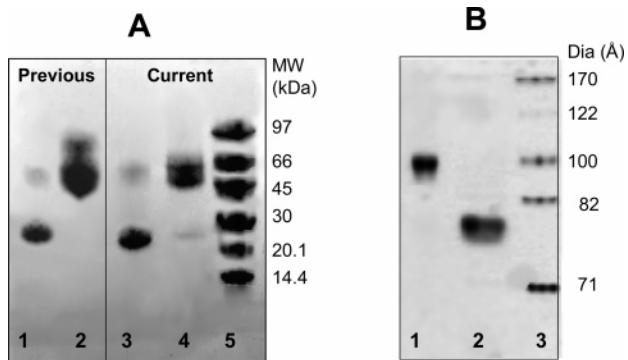


FIGURE 2: Discoidal particle characterization and separation of cross-linked rHDL into monomeric and dimeric apoA-I. Discoidal rHDL particles containing apoA-I were cross-linked with DSP or BS³, delipidated, and then separated by gel filtration chromatography. Panel A: 8–25% SDS Phast gel showing chromatographically separated cross-linked apoA-I monomer and dimer obtained in previous (DSP cross-linking) (14) and current (BS³ cross-linking) experiments of 96 Å rHDL particles. Cross-linked apoA-I monomer (lanes 1 and 3), cross-linked apoA-I dimer (lanes 2 and 4), and low molecular weight standards (lane 5). Panel B: ApoA-I discoidal rHDL particles as characterized on an 8–25% nondenaturing Phast gel prior to cross-linking. Lane 1: 96 Å particles. Lane 2: 78 Å particles. Lane 3: high molecular weight standards. Both gels were stained with Coomassie Blue.

assigned by mass mapping of experimental masses with a theoretically constructed list of all possible intra/intermolecularly cross-linked masses. A map was considered positive if the experimental and theoretical mass came within 50 ppm with the correct number of Lys residues available for the cross-linker formation. Moreover, as described in our previous paper in detail (14), it was assumed that trypsin does not cleave on the C-terminal side of cross-linker modified Lys residues, and only fully tryptically cleaved masses were considered as matches. To gain additional evidence for the

putative cross-link identifications, MS/MS analysis was performed on the most intense ion for each cross-link. See legend to Figure 3.

To distinguish between inter- and intramolecular cross-links, apoA-I that had been cross-linked in the discoidal rHDL was delipidated and then separated into two fractions on a gel filtration column. The first fraction contained dimeric apoA-I with at least one intermolecular cross-link, but likely more, and all possible intramolecular cross-links. The second fraction contained monomeric apoA-I that did not successfully form an intermolecular cross-link on the particles, but contained all possible intramolecular cross-links. By comparing the peptide masses from the dimeric sample to those from the monomeric sample it is theoretically possible to determine the intra- or intermolecular nature of a particular cross-link. However, despite our best efforts, it was not possible to completely eliminate small amounts of cross-contamination in the separation, i.e., there was a small amount of dimer in the purified monomer sample and a small amount of monomer in the purified dimer sample (Figure 2A). Because of the high sensitivity of the technique, it was still possible to detect masses that correspond to an intermolecular cross-link in the “monomeric” sample, although the intensity of these peaks was much lower in the monomeric sample vs the dimeric sample. To circumvent this problem, the ratio of intensities for 10–15 peptides that do not contain a lysine residue (and were therefore completely unaffected by the cross-linker) were compared between the dimeric and monomeric samples. In this experiment, the maximal intensity ratio of unmodified peptides between the dimeric and monomeric samples was 2.0. We reasoned that if the dimeric/monomeric ratio of cross-linked peptides was >2.0, then the mass is disproportionately represented in the dimeric sample and was defined as an intermolecular cross-link. Conversely,

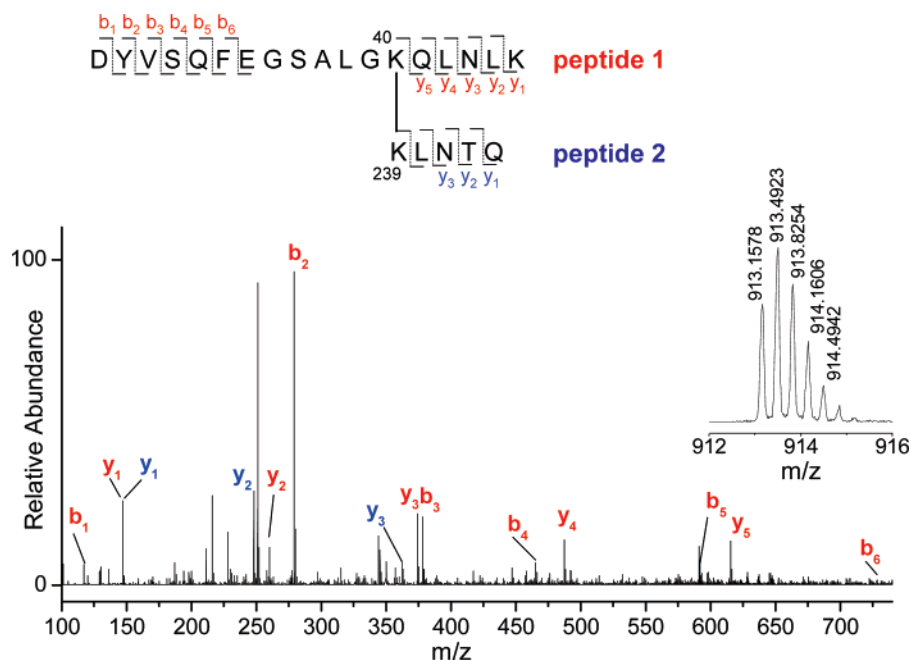


FIGURE 3: MS/MS evidence for the intermolecular cross-link K40–K239. MS/MS fragments (b-ions and y-ions) resulted from amide bond cleavage of the intermolecularly cross-linked peptide K40–K239 (MW 2736.4398) are labeled according to their single letter abbreviations. Several other typical fragments from the parent ion including immonium, b-NH₃, and y-NH₃ are present but are not indicated in order to reduce the complexity of the spectrum. The mass spectrum of the parent ion of K40–K239 peptide (charge state +3) is shown in the inset. The sequences of the two tryptic peptides involved in cross-linker formation are shown, with ions indicated in the spectrum highlighted. Only the lower end of the spectrum is shown for clarity.

Table 1: Cross-linked Peptide Masses Identified in a 96 Å rHDL Particle Cross-Linked with BS³

peptides involved		lysines involved	exp mass (Da)	deviation ^a (Da)	int ratio ^b	comment ^c	MS/MS evidence ^d
84–96		K88–K94	1671.84	0.00	1.7	intramolecular*	✓
95–107		K96–K106	1716.91	0.01	1.6	intramolecular*	✓
11–27		K12–K23	2015.10	0.01	1.4	intramolecular*	✓
227–243		K238–K239	2108.11	0.01	0.7	intramolecular*	
207–215x	207–215	K208–K208	2161.19	0.02	6.3	intermolecular	✓
1–10x	89–96	N _T –K94 ^e	2294.13	0.02	1.7	intramolecular	✓
89–106		K94–K96 ^f	2302.16	0.02	1.8	intramolecular*	✓
132–149		K133–K140 ^g	2302.20	0.00	1.4	intramolecular*	✓
196–215		K206–K208	2346.25	0.01	1.8	intramolecular*	✓
84–94x	117–123	K88–K118	2357.20	0.02	4.3	intermolecular	✓
107–116x	117–123	K107–K118	2417.32	0.08	1.6	intramolecular	✓
95–106x	117–123	K96–K118	2457.35	0.02	2.8	intermolecular	✓
28–45x	239–243	K40–K239	2736.42	0.02	2.7	intermolecular	✓
117–123x	134–149	K118–K140	2914.56	0.11	8.6	intermolecular	✓
84–94x	95–106	K88–K96	2923.59	0.14	1.6	intramolecular	✓
46–61x	207–215	K59–K208	3030.70	0.10	5.2	intermolecular	✓
216–238x	239–243	K226–K239	3337.96	0.15	6.5	intermolecular	
28–59		K40–K45	3728.04	0.18	1.4	intramolecular*	
46–61x	189–206	K59–K195	4046.22	0.16	8.9	intermolecular	
62–83x	189–206	K77–K195	4782.47	0.10	5.9	intermolecular	✓

^a Deviation is defined as the absolute value of the experimental mass – expected mass. ^b This refers to the ratio of intensity of a given mass found in the cross-linked dimer versus the same mass found in the cross-linked monomer experiment. A ratio of less than 2.0 indicated little change in the intensity of the mass between the two samples predicting an intramolecular cross-link. Ratios higher than 2.0 were assigned as an intermolecular cross-link, because the cross-link was prevalent in the dimer sample. See Experimental Procedures. ^c The cross-linked peptide masses denoted as “intramolecular*” have the cross-link within the same tryptic peptide. ^d MS/MS analysis was used for additional confirmation of putative cross-linked peptides. The masses indicated by “✓” have additional MS/MS evidence for at least a few consecutive fragment ions from the assigned putative peptide sequences. Peptides that do not have a check did not have a suitable fragmentation pattern for the analysis. Please refer to Figure 3 for a detailed example of the identification of peptide fragments. Note that the samples used in MS/MS analysis were processed using similar conditions described under Experimental Procedures except monomer–dimer separation after cross-linking. ^e N_T indicates the N-terminus NH₂ group of apoA-I. ^{f,g} Cross-links K94–K96 and K133–K140 with similar monoisotopic masses were distinguished and identified on the basis of their two different chromatographic elution times 6 min apart.

if this ratio was ≤ 2.0 , the mass was defined as an intramolecular cross-link. It is important to note that this ratio is variable from experiment to experiment and depends entirely on the amount of injected protein sample for the analysis (i.e., this ratio was 1.7 in our previous study (14)).

RESULTS AND DISCUSSION

Rationale and Approach. As mentioned above, our previous cross-linking study provided strong evidence that apoA-I adopts a belt-like conformation in 96 Å rHDL that aligns the amphipathic helices in a manner that matches the predictions from salt bridge stability analyses (12). However, we were unable to unequivocally discriminate between the double-belt or head-to-head hairpin models because we found cross-links that were unique to both models. We proposed that both arrangements may exist within a population of similar sized particles. However, the possibility remained that there was structural heterogeneity within our rHDL samples that led to ambiguous results. Figure 2A shows an 8–25% SDS–PAGE analysis of the 96 Å particles from our original study. When the discs were cross-linked, the predominant species formed were apoA-I monomers (Figure 2A, lane 1) and dimers (Figure 2A, lane 2) as expected. However, we also noticed that a small amount of trimer was present (Figure 2A, lane 2), even after the species were separated by gel filtration. We attributed this to the slight contaminating presence of larger discs that contain three molecules of apoA-I per particle (16). At the time, we did not believe that this minor species would affect our interpretation. However, after gaining additional experience with the technique and its sensitivity, we realized that it is possible

that the structure of the trimeric form may differ in some way from the predominant dimeric form, perhaps explaining our inability to distinguish between the models.

Therefore, we made several changes to our reconstitution procedure to increase the homogeneity of 96 Å complexes. First, we reduced the initial POPC to protein ratio from 90:1 to 78:1 and included a small amount of free cholesterol (5:1 cholesterol to protein) which we know from experience tends to increase particle homogeneity. The cross-linking was carried out immediately after obtaining homogeneous particles without giving them a chance to rearrange to differently sized particles. In addition, we refined our purification strategy to include two gel filtration columns in tandem (see Experimental Procedures) to better purify the complexes. Finally, to maximize detectible cross-links, we used a more stable cross-linking agent. Previously, we used DSP (spacer arm of 12 Å), which contains a reducible disulfide linkage in the spacer arm. Here, we used BS³, which has a similar spacer-arm length (11.4 Å) without the disulfide linkage. We consistently found that we were able to identify more cross-links in samples generated with BS³ for reasons that are not entirely clear.

96 Å Particle: Results. The outcome of these manipulations is shown in Figure 2A. It is clear that the 96 Å particles generated in this study lacked the trimeric contaminant in the cross-linked dimer sample that was present in our previous study (Figure 2A, lanes 4 vs 2). The high degree of homogeneity of these particles when analyzed by native PAGE is illustrated in Figure 2B, lane 1.

We identified 11 intramolecular cross-links and 9 intermolecular cross-links (Table 1) in the 96 Å particles. To

Table 2: Cross-Link Compatibility with Different Belt Models^a

intermolecular cross-links	double belt (5/5 orientation)	hairpin		Z-belt
		head-to-head	head-to-tail	
K208–K208	X	X	X	X
K88–K118	X	X	X	X
K96–K118	X	X	X	X
K40–K239	✓	✓	X	X
K118–K140	✓	X	X	X
K59–K208	✓	X	X	X
K226–K239	✓	✓	X	X
K59–K195	✓	X	X	X
K77–K195	✓	X	X	✓
compatibility	6/9	2/9	0/9	1/9

^a 10/11 intramolecular cross-linkers listed in Table 1 are compatible with all four belt models shown in Figure 1 whereas the remaining cross-linker, N_T–K94, is not compatible with any of the models.

increase the confidence that we have correctly identified the cross-linked peptides, we performed MS/MS analyses on peaks that we identified as cross-links from the molecular weight analysis described in Experimental Procedures. We were able to obtain MS/MS evidence that confirmed, at least partially, the amino acid composition of 7 of the 9 intermolecular cross-links (Table 1). An example of this analysis is shown in Figure 3. Therefore, taking into account (a) the reproduction of many of the cross-links in our previous study (allowing for differences in mass additions of the cross-linker), (b) the high mass accuracy of the instrumentation, (c) the high purity of the apoA-I preparations, and (c) the fragmentation evidence from the MS/MS analysis, the chances of misidentifying a cross-link are extremely remote. Furthermore, note that all 8 peptides in Table 1 containing intrapeptide cross-links, i.e., two lysines cross-linked within the same tryptic peptide (which therefore must be intramolecular), were correctly indicated to be intramolecular cross-links as judged by the intensity ratio analysis (see Experimental Procedures). Conversely, the K208 to K208 cross-

link occurring between the same Lys residue (which therefore must be intermolecular) was correctly identified as intermolecular.

Although many of the cross-links had been found previously, there were several new cross-links observed in this study. The K77–K195 and K118–K140 intermolecular cross-links which uniquely supported the double-belt model in our previous study were clearly present in the current study. In addition, we identified two new intermolecular cross-links, K59–K195 and K59–208, that also uniquely support the double-belt molecular arrangement (see below). One notable cross-link that was *not* observed was the intramolecular K45–K208. This was the only cross-link from our previous study that uniquely supported the existence of the hairpin structure.

96 Å Particle: Structural Implications. The abilities of the 9 intermolecular cross-links reported in Table 1 to qualitatively “fit” the models shown in Figure 1 are summarized in Table 2. Short range intramolecular cross-links were not informative in terms of protein backbone arrangement as they fit all the models equally well and hence are not listed in the table. One exception is the N_T–K94 cross-link that did not fit any model. At this point, the origin of this cross-link is not clear, although we would point out that this same connection appeared during our studies of the lipid-free form of apoA-I (17). As can be seen clearly, the intermolecular cross-links fit the models to dramatically different extents. Of the 9 intermolecular cross-links, none fit the head-to-tail hairpin model and only one fit the Z-belt orientation. However, 6 of the cross-links fit the 5/5 version of the double-belt model, whereas only 2 fit the head-to-head hairpin model. The fits for the latter two models are shown graphically in Figure 4. The observed intermolecular cross-link distances were tested more rigorously in silico using the LL5/5 (G129j) double-belt model (12, 18). Table 3 shows that the residues found to be in cross-links were

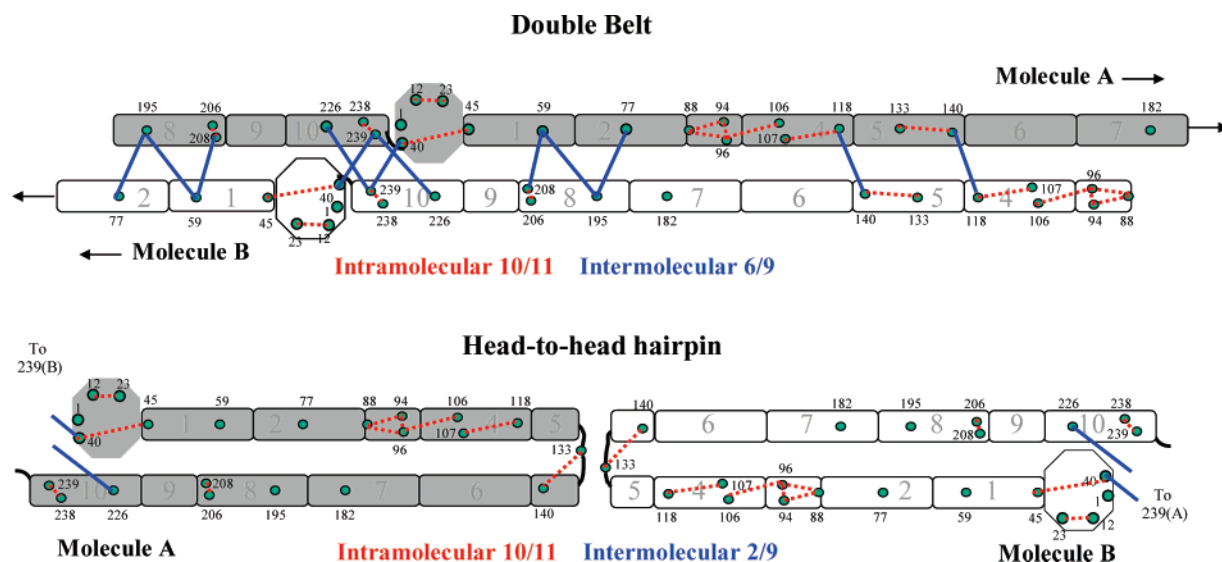


FIGURE 4: Schematic representation of experimentally observed cross-links with regard to the 5/5 (G129j) double-belt model and the head-to-head hairpin model for 96 Å particles containing two molecules of apoA-I. Two apoA-I molecules are shown in gray (molecule A) and white (molecule B). Each amphipathic helical segment of apoA-I is represented as a rectangle and is numbered according to the scheme of Roberts et al. (27). Approximate locations of the 21 lysine residues are given as dots with a number representing the location within the protein sequence. Intramolecular cross-links are shown in red, and intermolecular cross-links are shown in blue (listed in Table 1). The numbers of cross-links that fit each model with respect to total cross-links found (Table 2) are shown with the same color coding used in the scheme. Cross-links that do not obviously fit the model are not shown.

Table 3: Distance Calculations of Experimentally Identified Intermolecular Cross-Links with BS³ Using a Computer Model of the Double-Belt 5/5 (G129j) Rotamer in the LL and RR Stacking Interfaces^a

residues in cross-link ^b	theor dist between two lysines in the LL5/5 (G129j) rotamer (Å) ^c			theor dist between two lysines in the RR5/5 (G129j) rotamer (Å)		
	β-C to β-C	NH ₂ to NH ₂	possible?	β-C to β-C	NH ₂ to NH ₂	possible?
	β-C	NH ₂		β-C	NH ₂	
K208–K208	73	63	no	70	60	no
K88–K118	75	65	no	77	67	no
K96–K118	65	55	no	67	57	no
K118–K140	8	0	yes	17	7	yes
K59–K208	11	1	yes	12	2	yes
K226–K239	9	0	yes	11	1	yes
K59–K195	14	4	yes	22	12	borderline
K77–K195	15	5	yes	21	11	borderline

^a The model calculations were carried out using a 105 Å maximal Stokes diameter disc containing two apoA-I molecules (residues 44–243) in a circular planar antiparallel double-belt orientation. The LL or RR notation refers to left-to-left or right-to-right docking interfaces between the two molecules on the disc. The registry of the two molecules is termed “G129j” indicating the juxtaposition of G129 residues of each molecule. For more information on the concepts of docking interfaces and molecular registries, please see refs 12 and 18. ^b Note that the intermolecular cross-link K40–K239 (Tables 1 and 2) is not listed because the model used for calculations only contained residues 44–243. ^c Distances are shown with respect to both the distances between the β-carbons of the cross-linked residues and the distances from the terminal NH₂ groups because of the potential flexibility of the side chain. A cross-link is “possible” according to the model if the distance between two NH₂ groups of lysines are <11.4 Å (the spacer-arm length of BS³).

well within the allowed 11.4 Å spacer-arm distance in the model. Although considerably less favorable than the LL in terms of salt bridge potential, our data also fit the RR version of the 5/5 double belt (Table 3). However, all the distances between cross-linked residues are increased in the RR5/5 vs the LL5/5 model and two of the cross-links would have to stretch to the maximum length (11–12 Å) to accomplish the linkage. Therefore, the LL5/5 double-belt model is most consistent with our experimental data.

The disappearance of the intermolecular cross-link between K45 and K208 in this study suggests that this particular cross-link exists only when there is a third molecule of apoA-I on an HDL particle. This is intriguing in light of geometric constraints of the double-belt model. The double-belt idea works well for discs that contain two molecules of apoA-I per disc and can be applied to discs containing multiples of

Table 4: Distance Calculations of “Orphan” Intermolecular Cross-Links Using a Shifted Double-Belt Model LL5/2 (K206j)^a

residues in cross-link	theor dist between two lysines in the LL5/2 (K206j) rotamer ^b (Å)		
	β-C to β-C	NH ₂ to NH ₂	possible?
K208–K208	14	4	yes
K88–K118	6	0	yes
K96–K118	12	2	yes
K106–K106	20	10	yes

^a Model calculations were carried out as explained in Table 3 with the use of a shifted rotamer (LL5/2) in which helix 5 of molecule 1 aligns with helix 2 of molecule 2 and vice versa. LL5/2 is denoted as K206j due to juxtaposition of Lys residues at position 206 in this registry (18, 26). ^b A cross-link is “possible” according to the model if the distance between two NH₂ groups of lysines is <11.4 Å, the spacer-arm length of BS³.

two molecules. However, in discs containing 3 apoA-I, it is impossible to incorporate the third molecule without postulating that it folds back upon itself, as in a hairpin (12). Therefore, our data may support the presence of a third molecule of apoA-I in a hairpin orientation present in trimeric particles. Studies that directly compare discs with two and three apoA-I molecules per particle are required to confirm this hypothesis.

If particles with two molecules of apoA-I conform to the 5/5 double-belt model, then why are there some cross-links that do not fit the model? In both previous and current work, we observed the presence of a few cross-links (listed in Figure 5) that clearly do not fit the 5/5 double-belt (Table 2) or any other model in Figure 1. Interestingly, we found that all of these “orphan” cross-links could fit a variant of the double-belt model in which molecule A is slid two helical positions toward the N-terminus of molecule B, resulting in a LL5/2 molecular registry (Figure 5). Based on this, the computer model used to generate distances in Table 3 was modified to a LL5/2 (K206j) molecular registry with maximal salt bridge potential. Table 4 shows that all four cross-links were possible in the 5/2 orientation. The simplest explanation of this finding is that the molecules of apoA-I can slide in relation to each other on the edge of a disc, like wheels on a combination thumb lock. In fact, if one accepts the possibility that apoA-I exists as two populations in 5/5 and 5/2 orientations, then every single intermolecular cross-link that we observed in the current study would fit this model. Such a variable helical registry concept has precedence from fluorescence studies of apoA-I discs by Sorci-Thomas et al.

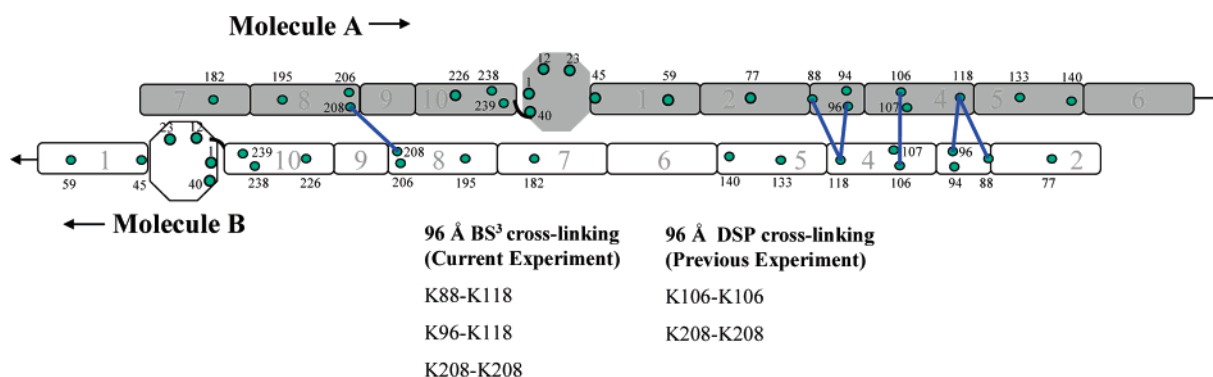


FIGURE 5: Schematic representation of shifted double belt (5/2 orientation) to accommodate incompatible intermolecular cross-links identified in BS³ and DSP cross-linking experiments. The layout of the figure is similar to that of Figure 4. The four intermolecular cross-links which do not fit the 5/5 double-belt model identified in either the BS³ or DSP experiment are shown in blue.

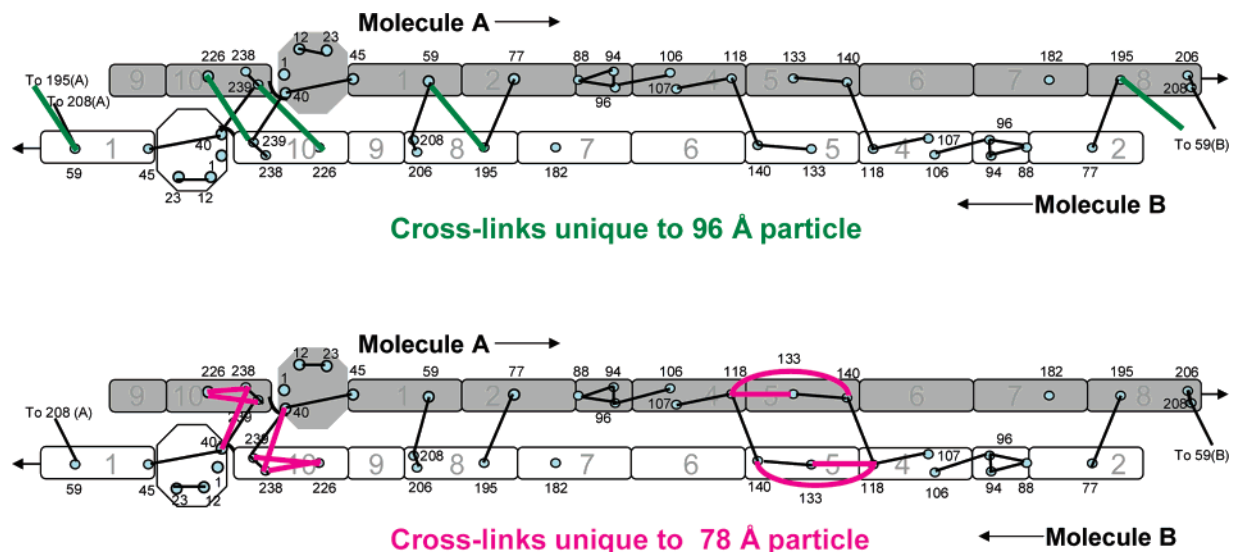


FIGURE 6: Comparison of cross-links identified in 78 Å particle vs 96 Å particle. The layout of the figure is identical to that of Figure 4. Both intra- and intermolecular cross-links that were not present in the 78 Å particle, but were in the 96 Å particle, are shown in green (top), whereas the cross-links unique to the 78 Å particle are shown in pink (bottom). Cross-links common to both particles are shown in black.

(19). If this is the case, we would speculate that the 5/5 form is the preferred conformation as it exhibited the highest number of cross-links. However, there are alternative explanations for the existence of the cross-links listed in Figure 5. For example, they could represent some transition state of apoA-I, perhaps as it exchanges between different particles. Indeed, the LL5/2 helical registry is not considered particularly stable when analyzed in terms of the number of potential salt bridge interactions occurring between the two molecules of apoA-I (12). Although the existence of a 5/2 double-belt conformer requires further verification, we find it a remarkable coincidence that every intermolecular cross-link that does not fit the 5/5 conformation fits the 5/2 model.

78 Å Particle: Results. In order to gain insight into the structural transitions within apoA-I when the particle diameter is changed, we generated a 78 Å particle that also contains two molecules of apoA-I. The high homogeneity of this particle is evident in Figure 2B (lane 2), and the separation of the monomeric cross-linked from the dimeric form was identical to that shown for the 96 Å particle (Figure 2A) with no trace of trimeric contaminant (data not shown). Figure 6 shows that many of the cross-links that we observed in the 96 Å particle were also present in the smaller disc (e.g., K40–K239, K59–K208, K118–K140, and K77–195). Interestingly, there were some cross-links that were unique to 96 Å particles as well as several that were unique to the 78 Å particles.

78 Å Particle: Structural Implications. When the diameter of an apoA-I containing discoidal complex is decreased, the protein annulus must decrease in order to maintain contact with the lipid. It has been proposed that apoA-I contains one or more “hinge” domains that are responsible for this surface area buffering effect (20, 21). The cross-links noted above clearly demonstrate that the overall form of the 5/5 double-belt model also appears to hold in the 78 Å particles. However, we found two major areas where cross-link changes were clustered. The first is near helix 5. In the 78 Å particle, we observed additional intramolecular cross-links forming between K118–K140 and K118–K133. This is consistent with a conformational change in this helix that

brings these residues closer together in the 78 Å particles. This could easily be visualized if the transition from a 96 Å particle to a 78 Å particle causes helix 5 to unfold from a helix to a random coil. Using independent methods, we have previously demonstrated that the helix 5 region is dissociated from the edge of a 78 Å disc when compared to the 96 Å particles (22). The second concentration of cross-link changes comes at the junction between the C-terminus and the N-terminus. Interestingly, Li et al. (18) recently provided solid evidence for the importance of the N-terminal 43 amino acids of apoA-I in the modulation of disc size heterogeneity. They proposed that the N-terminal domain, in conjunction with a more C-terminal domain such as helix 5, may act as hinge domains to modulate particle diameter. Our cross-linking data appears to support this proposal. However the data does not rule out other areas that may also change conformation. Preliminary results from molecular dynamic simulations (Segrest et al., unpublished data) support the possibility of substantial conformational changes of both apoA-I and lipids when lipids are limited.

In addition to the cross-links shown in Figure 6, there were four more intermolecular cross-links (K182–K238, K96–K118, K208–208, and K23–K94) that were consistently present in 78 Å particles that did not fit the 5/5 belt model. Three of these, however, are consistent with the 5/2 conformer, perhaps suggesting that variable registry can also occur in the smaller particles. The origin of the K23–K94 cross-link is not clear at this point.

CONCLUSION

Our previous studies provided the most comprehensive list of distance constraints obtained for lipid-bound forms of apoA-I. Using that data, we were able to argue against the significant contributions of the tail-to-tail hairpin and the “Z”-belt models for the structure of apoA-I on a disc. Using a refined experimental system, we now propose that the predominant conformation for two molecules of apoA-I on a disc closely resembles that predicted by the LL5/5 (G129j) double-belt model. However, it is possible that hairpin forms can exist, perhaps in particles containing odd numbers of

apoA-I per particle. Furthermore, we propose the possibility that a second stable form of the double belt may exist in a LL5/2 (K206j) conformer. If confirmed, the functional consequences of such a transition would be an exciting avenue of investigation. However, since the *in vivo* structure of discoidal HDL depends uniquely upon a complex and not yet understood process of lipid accumulation that requires minimally the transmembrane protein, ABCA1 (23–25), we would caution that the structure of *in vitro* discs may not entirely reflect circulating structures in plasma. The cross-linking approach should be well suited for testing models worked out on *in vitro* on actual particles isolated from human plasma.

REFERENCES

- Gordon, T., Castelli, W. P., Hjortland, M. C., Kannel, W. B., and Dawber, T. R. (1977) High density lipoprotein as a protective factor against coronary heart disease. The Framingham Study, *Am. J. Med.* **62**, 707–714.
- Tall, A. R. (1998) An overview of reverse cholesterol transport [Review], *Eur. Heart J.* **19** (Suppl. A), A31–A35.
- Asztalos, B. F. (2004) High-density lipoprotein metabolism and progression of atherosclerosis: new insights from the HDL Atherosclerosis Treatment Study, *Curr. Opin. Cardiol.* **19**, 385–391.
- Frank, P. G., and Marcel, Y. L. (2000) Apolipoprotein A-I: structure-function relationships, *J. Lipid Res.* **41**, 853–872.
- Segrest, J. P. (1977) Amphipathic helices and plasma lipoproteins: thermodynamic and geometric considerations, *Chem. Phys. Lipids* **18**, 7–22.
- Wlodawer, A., Segrest, J. P., Chung, B. H., Chioveti, R. J., and Weinstein, J. N. (1979) High-density lipoprotein recombinants: evidence for a bicycle tire micelle structure obtained by neutron scattering and electron microscopy, *FEBS Lett.* **104**, 231–235.
- Brouillette, C. G., Anantharamaiah, G. M., Engler, J. A., and Borhani, D. W. (2001) Structural models of human apolipoprotein A-I: a critical analysis and review, *Biochim. Biophys. Acta* **1531**, 4–46.
- Borhani, D. W., Rogers, D. P., Engler, J. A., and Brouillette, C. G. (1997) Crystal structure of truncated human apolipoprotein A-I suggests a lipid-bound conformation, *Proc. Natl. Acad. Sci. U.S.A.* **94**, 12291–12296.
- Koppaka, V., Silvestro, L., Engler, J. A., Brouillette, C. G., and Axelsen, P. H. (1999) The structure of human lipoprotein A-I. Evidence for the “belt” model, *J. Biol. Chem.* **274**, 14541–14544.
- Maiorano, J. N., and Davidson, W. S. (2000) The orientation of helix 4 in apolipoprotein A-I-containing reconstituted high density lipoproteins, *J. Biol. Chem.* **275**, 17374–17380.
- Panagotopoulos, S. E., Horace, E. M., Maiorano, J. N., and Davidson, W. S. (2001) Apolipoprotein A-I adopts a belt-like orientation in reconstituted high density lipoproteins, *J. Biol. Chem.* **276**, 42965–42970.
- Segrest, J. P., Jones, M. K., Klon, A. E., Sheldahl, C. J., Hellinger, M., De Loof, H., and Harvey, S. C. (1999) A detailed molecular belt model for apolipoprotein A-I in discoidal high density lipoprotein, *J. Biol. Chem.* **274**, 31755–31758.
- Brouillette, C. G., and Anantharamaiah, G. M. (1995) Structural models of human apolipoprotein A-I [Review], *Biochim. Biophys. Acta* **1256**, 103–129.
- Davidson, W. S., and Hilliard, G. M. (2003) The spatial organization of apolipoprotein A-I on the edge of discoidal high density lipoprotein particles: A mass spectrometry study, *J. Biol. Chem.* **278**, 27199–27207.
- Lund-Katz, S., and Phillips, M. C. (1986) Packing of cholesterol molecules in human low-density lipoprotein, *Biochemistry* **25**, 1562–1568.
- Wald, J. H., Krul, E. S., and Jonas, A. (1990) Structure of apolipoprotein A-I in three homogeneous, reconstituted high density lipoprotein particles, *J. Biol. Chem.* **265**, 20037–20043.
- Silva, R. A., Hilliard, G. M., Fang, J., Macha, S., and Davidson, W. S. (2005) A Three-Dimensional Molecular Model of Lipid-free Apolipoprotein A-I Determined by Cross-linking/Mass Spectrometry and Sequence Threading, *Biochemistry* **44**, 2759–2769.
- Li, L., Chen, J., Mishra, V. K., Kurtz, J. A., Cao, D., Klon, A. E., Harvey, S. C., Anantharamaiah, G. M., and Segrest, J. P. (2004) Double belt structure of discoidal high density lipoproteins: molecular basis for size heterogeneity, *J. Mol. Biol.* **343**, 1293–1311.
- Li, H. H., Lyles, D. S., Pan, W., Alexander, E., Thomas, M. J., and Sorci-Thomas, M. G. (2002) ApoA-I structure on discs and spheres. Variable helix registry and conformational states, *J. Biol. Chem.* **277**, 39093–39101.
- Brouillette, C. G., Jones, J. L., Ng, T. C., Kercret, H., Chung, B. H., and Segrest, J. P. (1984) Structural studies of apolipoprotein A-I/phosphatidylcholine recombinants by high-field proton NMR, nondenaturing gradient gel electrophoresis, and electron microscopy, *Biochemistry* **23**, 359–367.
- Jonas, A., Kezdy, K. E., and Wald, J. H. (1989) Defined apolipoprotein A-I conformations in reconstituted high density lipoprotein discs, *J. Biol. Chem.* **264**, 4818–4824.
- Maiorano, J. N., Jandacek, R. J., Horace, E. M., and Davidson, W. S. (2004) Identification and structural ramifications of a hinge domain in apolipoprotein A-I discoidal high-density lipoproteins of different size, *Biochemistry* **43**, 11717–11726.
- Bodzioch, M., Orso, E., Klucken, J., Langmann, T., Bottcher, A., Diederich, W., Drobnik, W., Barlage, S., Buchler, C., Porsch-Ozcuremez, M., Kaminski, W. E., Hahmann, H. W., Oette, K., Rothe, G., Aslanidis, C., Lackner, K. J., and Schmitz, G. (1999) The gene encoding ATP-binding cassette transporter 1 is mutated in Tangier disease, *Nat. Genet.* **22**, 347–351.
- Brooks-Wilson, A., Marzil, M., Clee, S. M., Zhang, L. H., Roomp, K., van Dam, M., Yu, L., Brewer, C., Collins, J. A., Molhuizen, H. O., Loubser, O., Ouellette, B. F., Fichter, K., Ashbourne-Excoffon, K. J., Sensen, C. W., Scherer, S., Mott, S., Denis, M., Martindale, D., Frohlich, J., Morgan, K., Koop, B., Pimstone, S., Kastelein, J. J., and Hayden, M. R. (1999) Mutations in ABC1 in Tangier disease and familial high-density lipoprotein deficiency, *Nat. Genet.* **22**, 336–345.
- Rust, S., Rosier, M., Funke, H., Real, J., Amoura, Z., Piette, J. C., Deleuze, J. F., Brewer, H. B., Duverger, N., Deneffe, P., and Assmann, G. (1999) Tangier disease is caused by mutations in the gene encoding ATP-binding cassette transporter 1, *Nat. Genet.* **22**, 352–355.
- Gillotte, K. L., Zaiou, M., Lund-Katz, S., Anantharamaiah, G. M., Holvoet, P., Dhoest, A., Palgunachari, M. N., Segrest, J. P., Weisgraber, K. H., Rothblat, G. H., and Phillips, M. C. (1999) Apolipoprotein-mediated plasma membrane microsolubilization. Role of lipid affinity and membrane penetration in the efflux of cellular cholesterol and phospholipid, *J. Biol. Chem.* **274**, 2021–2028.
- Roberts, L. M., Ray, M. J., Shih, T. W., Hayden, E., Reader, M. M., and Brouillette, C. G. (1997) Structural analysis of apolipoprotein A-I: limited proteolysis of methionine-reduced and -oxidized lipid-free and lipid-bound human apo A-I, *Biochemistry* **36**, 7615–7624.

BI050421Z